

Evolution of Class-Specific Peptides Targeting a Hot Spot of the G α s Subunit

Ryan J. Austin¹, William W. Ja² and Richard W. Roberts^{1*}

¹Departments of Chemistry and Biology, and Mork Family Department of Chemical Engineering/Materials Science, University of Southern California, Los Angeles, CA 90089, USA

²Division of Biology, California Institute of Technology, Pasadena, CA 91125, USA

Received 3 October 2007;
received in revised form
20 December 2007;
accepted 14 January 2008
Available online
18 January 2008

The four classes of heterotrimeric G-protein α subunits act as molecular routers inside cells, gating signals based on a bound guanosine nucleotide (guanosine 5'-triphosphate *versus* guanosine 5'-diphosphate). Ligands that specifically target individual subunits provide new tools for monitoring and modulating these networks, but are challenging to design due to the high sequence homology and structural plasticity of the G α -binding surface. Here we have created an mRNA display library of peptides based on the short G α -modulating peptide R6A-1 and selected variants that target a convergent protein-binding surface of G α s·guanosine 5'-diphosphate. After selection/evolution, the most G α s-specific peptide, G α s(s)-binding peptide (GSP), was used to design a second-generation library, resulting in several new affinity- and selectivity-matured peptides denoted as mGSPs. The two-step evolutionary walk from R6A-1 to mGSP-1 resulted in an 8000-fold inversion in binding specificity, altered seven out of nine residues in the starting peptide core, and incorporated both positive and negative design steps. The resulting mGSP-1 peptide shows remarkable selectivity and affinity, exhibiting little or no binding to nine homologous G α subunits or human H-Ras, and even discriminates the G α s splice variant G α s(l). Selected peptides make specific contacts with the effector-binding region of G α , which may explain an interesting bifunctional activity observed in GSP. Overall, our work demonstrates a design of simple, linear, highly specific peptides that target a protein-binding surface of G α s and argues that mRNA display-based selection/evolution is a powerful route for targeting protein families with high class specificity and state specificity.

© 2008 Elsevier Ltd. All rights reserved.

Keywords: mRNA display; directed evolution; G protein; convergent binding site; hot spot

Edited by J. Karn

Introduction

The heterotrimeric G-protein signaling pathway plays a central role in both biology and human

*Corresponding author. E-mail address: richrob@usc.edu.

Abbreviations used: GSP, G α s(s)-binding peptide; GPCR, G-protein-coupled receptor; GDP, guanosine 5'-diphosphate; GTP, guanosine 5'-triphosphate; GPR, G-protein-regulatory; GoLoco, G α (i/o)-Loco interaction; RGS, regulator of G-protein signaling; MBP, maltose-binding protein; mGSP, matured GSP; SPR, surface plasmon resonance; AlF₄, aluminum fluoride; AC, adenylyl cyclase; GTP γ S, guanosine 5'-O-(3-thiotriphosphate); GEF, guanine nucleotide exchange factor; PBS, phosphate-buffered saline; dsDNA, double-stranded DNA; EDTA, ethylenediaminetetraacetic acid; BSA, bovine serum albumin; RT, reverse transcription; cpm, counts per minute.

therapies. In this pathway, heterotrimeric G-protein subunits (denoted G α , β , and γ) route information from cell surface G-protein-coupled receptors (GPCRs) to specific intracellular effectors. Presently, GPCRs comprise the largest family of receptor drug targets in humans, accounting for 25% of marketed pharmaceuticals.¹ Routing of a signal from a GPCR to corresponding effectors is dictated by the identity of the G-protein α and $\beta\gamma$ heterodimer subunits associated with the GPCR. In humans, there is substantial combinatorial diversity in the routing partners, with 16 distinct G α subunit genes categorized into 4 classes (i/o, q/11, s, and 12/13) corresponding to their effector coupling, 5 β subunits, and 12 receptor-specific γ subunits.² Combinations of these components enable differentiated cells to respond uniquely to extracellular signals.³

While drugs targeting effector proteins do exist, so far, only one therapy, suramin, appears to target the G-protein routers themselves, inhibiting dissociation of nucleotide from $G\alpha \cdot$ guanosine 5'-diphosphate (GDP).^{4,5} One reason for this paucity of drugs arises from the difficulty of targeting large protein-protein binding interfaces with traditional drug-like molecules.⁶ Towards this end, our laboratory is interested in exploring whether peptides that recognize such surfaces with protein-like affinity and selectivity can be designed. We have investigated this concept in the context of the G-protein α subunits, with the goal of determining whether $G\alpha$ class- and state-specific peptide ligands that target the protein-binding surface of this router can be generated.

$G\alpha$ subunits comprise two domains: a unique helical domain and a GTPase domain containing the guanosine-nucleotide-binding pocket of the protein (Fig. 1a). The identity of the nucleotide bound within this pocket [guanosine 5'-triphosphate (GTP) versus GDP] is coupled to the conformation of the subunit's binding surface via three malleable switch elements in the GTPase domain (SI, SII, and SIII). This conformational "switching" provides the basis for $G\alpha$ router activity, allowing the subunit to bind different partners in its "on" ($G\alpha \cdot$ GTP) and "off" ($G\alpha \cdot$ GDP) states.

In the "off" state, $G\alpha \cdot$ GDP binds $G\beta\gamma$, forming a heterotrimer associated with the cytosolic face of the GPCR. Signal activation of the GPCR triggers exchange of GDP for GTP in $G\alpha$ and causes dissociation of $G\beta\gamma$. Both activated $G\alpha \cdot$ GTP and $G\beta\gamma$ are then capable of regulating effector response for a period of time, dependent upon the GTPase rate of $G\alpha$. GTP hydrolysis returns $G\alpha$ to its "off" state, resulting in reformation of the $G\alpha \cdot$ GDP- $G\beta\gamma$ heterotrimer and termination of signal.⁹ Beyond $G\beta\gamma$, which binds the "off" state of $G\alpha$, and various effector proteins that bind the "on" state, additional regulatory proteins also interact with the binding surface of $G\alpha$ in a conformation-specific manner. These include G-protein-regulatory (GPR) [$G\alpha(i/o)$ -Loco (GoLoco)] motifs, which are thought to sequester $G\alpha \cdot$ GDP and regulator of G-protein signaling (RGS) proteins that accelerate the rate of $G\alpha$ GTPase activity.¹⁰

The $G\alpha$ binding interfaces of these proteins have been shown to overlap at a convergent binding surface defined by switch II and α -helix 3 elements of the subunit (SII/ α 3).¹¹⁻¹³ Attributes of convergent binding surfaces, or binding "hot spots," were originally characterized by Clackson and Wells and have since been identified in a growing number of proteins.^{14,15} Such sites generally exhibit a hydrophobic character with a high degree of sequence conservation across different members of a protein family, as well as structural plasticity. Sequence conservation of the SII/ α 3 convergent binding site across various classes of the $G\alpha$ family is illustrated in Fig. 1b. This primary sequence identity results in highly conserved $G\alpha$ protein structures with a backbone RMSD of ~ 1 Å in the GTPase domains of $G\alpha i1$, $G\alpha q$, $G\alpha s(s)$, and $G\alpha 12$ subunits.^{8,11,16}

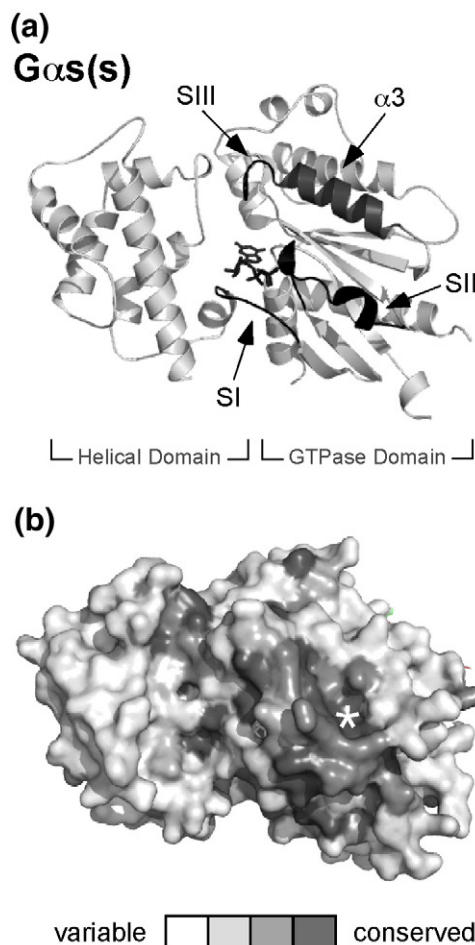


Fig. 1. Targeting the $G\alpha$ SII/ α 3 site. (a) Ribbon structure representation of the $G\alpha s(s)$ subunit. Malleable switch regions (SI, SII, and SIII) are depicted in black, with the bound nucleotide and α -helix 3 (α 3) in slate. The SII/ α 3 site of the subunit presents a convergent protein-binding surface that participates in a number of different protein-binding interactions. (b) Molecular surface representation of $G\alpha$ protein sequence homology superimposed on the $G\alpha s(s) \cdot$ GTP γ S crystal structure. A sequence alignment of $G\alpha$ proteins (i1, i2, i3, oA, q, 11, 15, s(s), Olf, and 12) was performed with ClustalW,⁷ generating a list of variable (near white), similar (light gray), conserved (gray), and identical (slate) $G\alpha$ residues, which were grafted onto the $G\alpha s(s) \cdot$ GTP γ S crystal structure. The asterisk denotes an invariant hydrophobic binding pocket within the SII/ α 3 cleft. Structural images were made from Protein Data Bank (PDB) file 1AZT⁸ using PyMOL [<http://www.pymol.org>].

The design of specific ligands that target convergent binding surfaces presents an interesting problem due to the sequence conservation and dynamic topography of these sites. Combinatorial approaches such as *in vitro* selection provide a powerful solution for targeting these molecularly compliant surfaces.¹⁷ Using such methods, our laboratory and others have previously developed a number of peptides that bind the SII/ α 3 site of $G\alpha$ in a conformation- and state-specific manner.^{13,18-20} In these selection experiments, a library of randomized peptide sequences

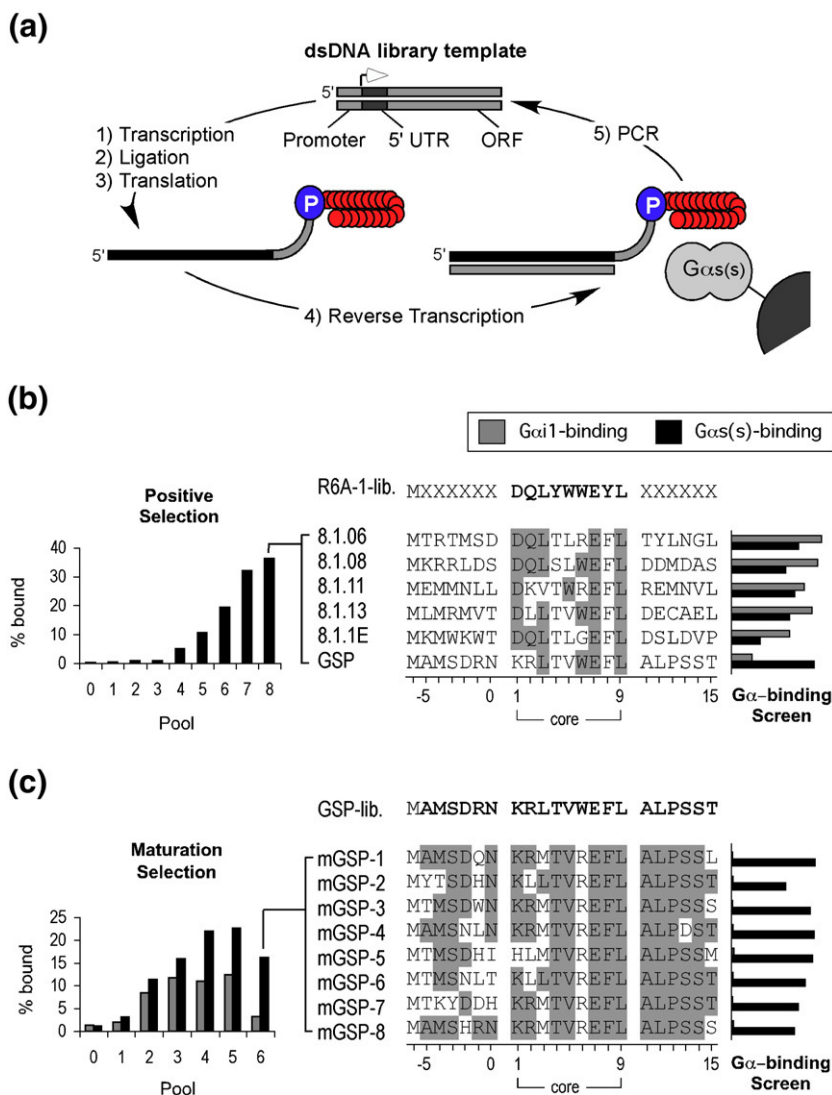
is selected for the ability to bind the G-protein target, typically using affinity chromatography. Functional sequences that bind the target are retained, are amplified, and eventually come to dominate the pool after iterative rounds of selection. The selection technique most often employed by our laboratory is mRNA display, wherein each peptide in a library is covalently coupled to its encoding mRNA as an mRNA-peptide fusion (Fig. 2a).²¹ This approach allows libraries to be created entirely *in vitro*, that are strictly monovalent, and have sequence diversities of $>10^{13}$ independent polypeptide sequences, the most of any available method.²² Generally, mRNA display selections result in peptides that bind protein or nucleic acid targets with nanomolar to picomolar affinities.^{23–28}

In the present work, we have set out to determine whether it is possible to generate peptide modulators towards the SII/α3 site that are capable of discriminating the highly conserved subunit classes (i/o, q/11, s, and 12/13). Taking as our starting point

a short peptide known to bind the SII/α3 site of Gαi1, we have selected peptides targeting the short isoform of Gαs (Gαs(s)). Notably, our directed evolution strategy required both positive and negative selection steps, with the first step improving affinity for Gαs and with the second step removing binding to other Gα subunits. The resulting peptides are remarkably specific, showing no binding to the other three classes of Gα and even discriminating between the long and the short isoforms of Gαs. These peptides indicate that it is possible to modulate the SII/α3 site of Gα with class-specific ligands and illustrate a selection-based evolution of peptide binding specificity at a convergent binding site.

Results and Discussion

The immediate goal of our present work has been to select specific peptide ligands for the therapeutically



(c) Scheme for maturation selection (GSP library: Gαs(s) beads with Gαi1 competitor). On the left, enrichment of pool binding to Gαs(s) beads (black vertical bars) is contrasted with binding to Gαi1 beads (gray vertical bars). On the right, selected peptides from pool 6 bind specifically to Gαs(s) in the Gα binding screen.

Fig. 2. Directed evolution selection scheme. (a) mRNA display selection cycle. A dsDNA library (pool 0) containing an invariant T7 promoter, an untranslated region, and an open reading frame was synthesized. Template DNA was transcribed (1), ligated to puromycin via a 3'-DNA tether (2), and translated (3) to generate mRNA-peptide fusions, individually composed of a peptide (red) linked to its corresponding mRNA genotype (black) via puromycin (blue). Purified fusions are reverse-transcribed (4) prior to selection on a solid-phase target (Gαs(s) beads). PCR amplification of cDNA retained on the target (5) produces dsDNA template (pool 1) for the subsequent round of selection. (b) Scheme for positive selection (R6A-1 library: Gαs(s) beads). The R6A-1 library sequence is listed; residues in bold were doped with a 50% mutation rate, and random residues are represented as X's. On the left is a plot of pool enrichment for the positive selection: RNase-treated [³⁵S]Met-peptide fusions from iterative rounds of selection were assayed for pull down on Gαs(s) beads (black vertical bars) with background binding to neutravidin beads at <0.5%. On the right, individual peptide sequences from pool 8 were screened for their ability to bind soluble Gαi1 (gray horizontal bars) and Gαs(s) (black horizontal bars). Conserved residues in selected peptides are boxed in gray.

relevant Gas(s) protein target. More broadly, we are interested in exploring the nature and evolvability of molecular recognition between nominally structured peptide sequences and protein-binding surfaces. To this end, we have chosen the core peptide R6A-1, which binds the SII/ α 3 site of G α with a 250-fold preference for the G α i1 target over Gas(s),^{29,30} as a starting point for our present selection. Based on previous work demonstrating that the specificity of R6A-1 could be altered by the addition of flanking residues, we synthesized DNA oligonucleotides coding for an R6A-1-based library of peptides. This R6A-1 library was designed to incorporate a 40–50% doped (50–60% mutation rate per amino acid) R6A-1 peptide core flanked by random amino acid hexamers (Fig. 2b).²⁰ We expressed the library as a pool of mRNA–peptide fusions containing 1.6×10^{13} independent peptide sequences in pool 0 (see Materials and Methods).

Positive selection of the Gas(s)-binding peptide

To isolate Gas(s)-binding peptide sequences within the R6A-1 library, a positive selection of the library was performed on neutravidin beads coated with N-terminally biotinylated Gas(s) (Gas(s) beads). Here the positive selective pressure was binding to Gas(s). mRNA–peptide fusions from the pool that were retained on the Gas(s) beads were amplified by PCR and again expressed as mRNA–peptide fusions for subsequent rounds of selection. Enrichment of Gas(s)-binding sequences was observable after four rounds and plateaued after eight rounds of the positive selection, as measured by pull down of [³⁵S]Met-labeled peptide fusions on Gas(s) beads (Fig. 2b). Discrete peptide sequences from pool 8 were cloned and expressed as biotinylated peptide–maltose-binding protein (MBP) fusions. These peptide–MBP fusions were individually immobilized on neutravidin beads (peptide beads) and screened for binding to soluble [³⁵S]Met-labeled G α i1 and Gas(s) using a previously developed *in vitro* binding assay.²⁹

The majority of pool 8 peptide sequences screened retain an affinity for G α i1 equal to or greater than their affinity for Gas(s) in the G α binding screen. However, on Gas(s)-binding peptide (GSP), representing 5% of the pool 8 sequences screened, binds preferentially to Gas(s). In evaluating the selected round 8 sequences, we found only a fraction of the R6A-1 core residues to be conserved. A hydrophobic leucine or valine residue is conserved at position 3 of the selected clones, along with residues glutamate-phenylalanine-leucine (EFL) at positions 7–9 of the core.

Many of the enriched peptide sequences contain three to four nonconservative mutations in their core. The selected GSP sequence, for instance, contains five mutations within the nine-residue core, three of which are of low likelihood [D1K (0.7%); Y4T (1.0%); W5V (1.0%)] based on the theoretical complexity of our pool. The mutagenic probability of finding the GSP core in the R6A-1 library is

1.9×10^{-10} , meaning that in our 16-trillion-molecule pool 0, roughly 800 full-length copies of the GSP core were present. This copy number is too low to effectively sample the flanking sequences of the R6A-1 library, which may explain why a separate selection of the R6A-1 library in the presence of G α i1 competitor was unsuccessful (data not shown).

Maturation selection of Gas(s)-specific mGSPs

To explore GSP variants with increased Gas(s) binding specificity, a GSP library based on a 50% doped GSP sequence was constructed and subjected to a maturation selection (Fig. 2c). This maturation selection was designed to incorporate negative selective pressures against peptides that bind to G α i1. GSP variants were selected for retention on Gas(s) beads in the presence of a molar excess of soluble G α i1 competitor, with the concentration of G α i1 competitor and other negative selective pressures increasing over the course of the maturation selection (see Materials and Methods). After six rounds of selection, the majority of GSP variants sequenced bound exclusively to Gas(s) in the G α binding screen (Fig. 2c).

These matured GSP (mGSP) peptide variants retain the EFL motif, along with the GSP core residues K1, T4, and V5. As in the positive selection, we again observe significant mutations in the core sequence. In particular, peptides that display the greatest Gas(s) selectivity in the G α binding screen have an arginine residue at position 6 and either a methionine residue at position 3 (in mGSP-1) or a leucine residue at position 2 (in mGSP-2) of the core (Fig. 2c). The average number of GSP mutations in these mGSP variants is 5.7 ± 1.3 residues, a mutational distance that is covered by only one to four copies of each variant in the GSP library pool 0. This significant mutational distance suggests that additional selections could generate peptides with even greater Gas(s) binding specificities. Representative peptide variants mGSP-1 (mut: L3M) and mGSP-2 (mut: R2L), along with GSP, were synthesized for further analysis.

An 8000-fold specificity change in mGSP-1 and mGSP-2 compared to R6A-1

We have used surface plasmon resonance (SPR) to measure dissociation constant (K_d) values for a matrix of peptide–G α complexes between GSP, mGSP-1, and mGSP-2 peptides, and G α i1 and Gas(s) proteins (Fig. 3, Table 1). The K_d matrix charts the course of our two-selection step walk. (1) In the positive selection, we evolved peptides with increased Gas(s) affinity, walking through sequence space from the G α i1-specific R6A-1 peptide to GSP, which exhibits affinity for both G α i1 and Gas(s) proteins. (2) In the maturation selection, we applied a negative G α i1-selective pressure to the GSP library, evolving GSP variants that retained affinity for Gas(s) but no longer bound G α i1. Gas(s) binding specificities are quantified in Table 1 as the relative free-energy stability of

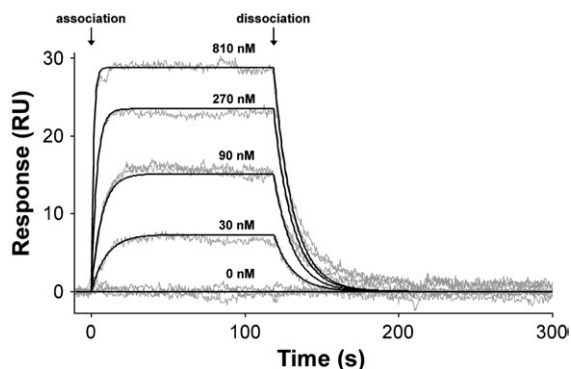


Fig. 3. SPR binding data for the GSP–Gas(s) complex. A concentration series of GSP was injected (200 μ l at 0 s, with a 100- μ l/min flow rate) across \sim 1000 response units of Gas(s) immobilized on a streptavidin biosensor chip. Global kinetic fits (black) are overlaid on the sensogram data (gray). Two sensogram plots at 90 nM GSP and three plots at 0 nM demonstrate data precision. The derived binding constant is shown in Table 1.

Table 1. Peptide–G α dissociation constants (K_d) and Gas(s) binding specificity [Gas(s)– $\Delta\Delta G$] values

Peptide	K_d (nM)		Gas(s)– $\Delta\Delta G$ (kcal/mol)
	G α i1	G α s(s)	
R6A	60		
R6A-1	200	50,000	–3.3
GSP	280 \pm 40	100 \pm 15	0.5
mGSP-1	10,300	300	2.1
mGSP-2	4400 \pm 220	130	2.1

K_d values, calculated from kinetic parameters (k_d/k_a), are given \pm SD when more than one independent measurement has been made. Gas(s)– $\Delta\Delta G$ values are calculated as Gas(s)– $\Delta\Delta G$ = [ΔG° (peptide–G α i1) – ΔG° (peptide–G α s(s))], where ΔG° = –RT ln K_{obs} .

R6A and R6A-1 binding constants are previously published values.^{18,29} The R6A peptide sequence is MSQTKRLD DQLYWWEYL.

the peptide–Gas(s) complex *versus* the peptide–G α i1 complex [Gas(s)– $\Delta\Delta G$]. In sum, the mGSP-1 and mGSP-2 peptides exhibit a 5.4-kcal/mol increase in Gas(s) binding specificity over R6A-1, equivalent to a >8000-fold inversion in G α i1/Gas(s) target discrimination.

G α class recognition by GSP, mGSP-1, and mGSP-2 peptides

We were expressly interested in evaluating the binding specificity of GSP and mGSP variants across the spectrum of G α subunits. To address this question, a palette of 11 different [³⁵S]Met-labeled G α subunits and isoforms (G α : i1, i2, i3, oA, q, 11, 15, s(s), s(l), Olf, and 12) representing the four classes of G α (i/o, q/11, s, and 12/13), as well as the small GTPase H-Ras, was expressed *in vitro* and assayed for pull down on peptide beads. The result was a G α class specificity profile for each peptide tested (Fig.

4). Here three experimental controls are worth noting. Firstly, pull-down reactions were performed in the presence of reticulocyte lysate, which acts as a general binding competitor, mimicking the cytosolic environment of the cell. Secondly, the presence of aluminum fluoride (AlF₄) in control pull-down experiments abrogated all bindings between G α subunits and the GSP, mGSP-1, and mGSP-2 peptides. This finding is consistent with state-specific binding of peptides to the GDP conformation of G α as previously reported for R6A-1.¹⁸ Finally, the ratio of G α i1 to Gas(s) binding in the specificity profile of GSP was consistent with the SPR data for the peptide (Fig. 4a).

The specificity profiles of GSP, mGSP-1, and mGSP-2 peptides illustrate novel recognition properties of these peptides that have resulted from the two-step directed evolution strategy of our selection. GSP, isolated from the initial positive selection, has a surprisingly focused binding profile, recognizing both i/o and s subunit classes, with only nominal affinity towards q/11 and 12/13 (Fig. 4a). This specificity is further pronounced in the mGSP-1 and mGSP-2 variants, isolated from the subsequent maturation selection step, which bind only the s class of G α subunits. Our results demonstrate that it

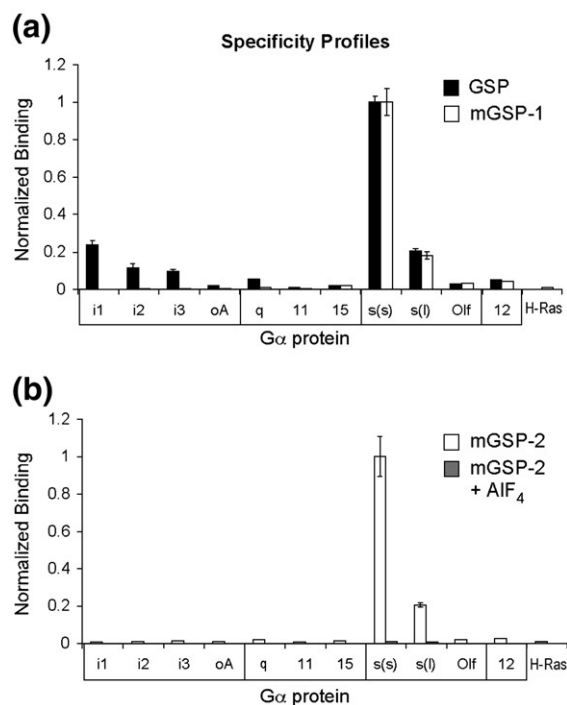


Fig. 4. G α binding specificity profiles. (a) GSP and mGSP-1 peptides were assayed for binding to a profile of 11 G α proteins and the small GTPase H-Ras, boxed by class along the x-axis of the plot. Binding is a measure of [³⁵S]Met-G α protein pull down on peptide beads performed at 4 $^\circ$ C. Control pull down on MBP-neut beads showed no binding (<0.01), and the presence of AlF₄ abrogated pull down for both peptides. Error bars represent SD for multiple experiments. (b) A specificity profile similar to mGSP-1 is shown for the mGSP-2 peptide, along with measurements performed in the presence of AlF₄.

is possible to evolve new Gα binding specificity in a peptide sequence without increasing the binding promiscuity of the peptide for other Gα classes. Indeed, even class subspecificity is apparent in selected peptides. GSP, mGSP-1, and mGSP-2 all show reduced binding to the long isoform of Gαs (Gαs(l)) and minimal binding to the GαOlf subunit, which shares a 77% amino acid sequence identity with Gαs(s).

Directed evolution experiments that evolve binding promiscuity or nonspecificity in an initial step before honing specificity in a subsequent step are often employed in cases where investigators cannot effectively sample the sequence space of large protein libraries.³¹ However, the number of possible amino acid combinations in a 21-residue peptide ($20^{21} = 2.1 \times 10^{27}$) is much smaller than that for a larger 100-residue protein ($20^{100} = 1.3 \times 10^{130}$), allowing for a more comprehensive search of amino-acid sequence space in peptide-directed evolution experiments. In our case, by taking the R6A-1 peptide as our starting point and by constructing doped peptide libraries, we have targeted our selection to the SII/α3 site of Gα, facilitating an even denser interrogation of peptide sequence space than afforded by a random 'naïve' peptide selection.

Sequence conservation between R6A-1 and the GSP and mGSP variants indicates that the selected peptides bind in a similar fashion to the SII/α3 site of Gα. This binding site redundancy is supported by our finding that R6A-1 directly competes with GSP for binding to Gαi1 (data not shown). Additionally, the GSP, like R6A-1, inhibits formation of the Gαβγ heterotrimer, reiterating our previous finding that peptides targeting the SII/α3 site can disrupt large protein-protein interactions.²⁹ [³⁵S]Gβγ pull down on both Gαi1 and Gαs(s) beads is inhibited by the presence of GSP at IC₅₀ values of 550 nM and 80 nM, respectively (Supplementary Fig. A).

GSP and mGSP-1 discriminate the effector-binding region of Gαs(s)

We designed our selection to target Gαs(s) at the SII/α3 site, which is a convergent protein interaction surface for a number of natural Gα-binding partners. Presently, four models of Gα binding specificity have been developed from structural characterization of Gα complexes that involve critical contacts within the SII/α3 site. These models are delineated by the classification of Gα-binding partner: (1) RGS proteins,^{32,33} (2) the GPR/GoLoco motif,³⁴ (3) effector proteins,^{11,12} and (4) Gβγ heterodimers.³⁵ A general theme that emerges from the models is that molecular recognition of Gα is bipartite, involving conserved contacts along the SII/α3-binding surface that are complemented by specific contacts outside of the SII/α3 site. RGS proteins provide a notable exception to this theme, making highly specific contacts at a nonconserved residue (Gαi1-Ser206) within switch II. To compare the binding specificity of GSP and mGSP variants with that of structurally characterized models, we have expressed a series of pre-

viously studied Gαi1/Gαs(s) reciprocal mutants^{36,37} and chimeras³⁸ and tested them for binding to peptide beads. Gα-binding footprints for RGS4, GoLoco, and the effector protein adenylyl cyclase (AC) are shown in Fig. 5a. The Gβγ-binding model, however, is not considered in our analysis, as relevant mutants and chimeras have not been characterized.

We considered the three remaining models in turn. (1) In the RGS-binding model, polar residues from RGS proteins discriminate the primary structure of Gα switches at five positions.^{32,33} Reciprocal substitution at one of these positions, Ser206 in Gαi1, with the corresponding residue, Asp229 from Gαs(s), abrogates binding of Gαi/o-specific RGS proteins.^{33,36,37} Similarly, the Asp229 position of Gαs(s) has been implicated in the Gαs-specific binding of RGS-PX1.³⁹ Binding of GSP and mGSP-1 peptides is not, however, affected by G-protein reciprocal substitutions at this position (Fig. 5b),

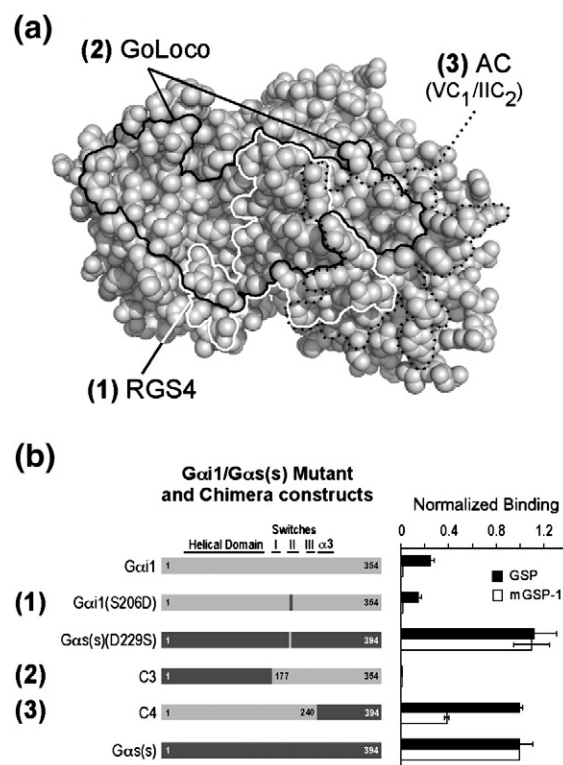


Fig. 5. Gα class recognition models. (a) Superimposition of (1) RGS (RGS4:³² dotted black line), (2) GoLoco (GPR/GoLoco:³⁴ black line), and (3) effector (AC VC₁/IIC₂:⁸ white line) binding footprints on Gα. The footprints overlap at the conserved SII/α3 site of Gα. Binding surfaces were grafted onto the Gαs(s) structure, PDB 1AZT;⁴ the image was generated by PyMOL [www.pymol.org]. (b) Mutational analysis. Previously characterized Gαi1/Gαs(s) reciprocal mutants and chimeras were assayed for pull down on GSP and mGSP-1 peptide beads. GSP and mGSP-1 exhibit increased binding to the C4 chimera containing the α3 and α3-β5 effector loop of Gαs(s). Chimera constructs are depicted on the left and denoted by respective binding models 1-3.³⁸ The constructs of Gαi1 sequence are shown in light gray; the Gαs(s) sequence, numbered in the Gαs(l) convention, is shown in dark gray.

indicating that the mechanism of peptide specificity is distinct from RGS binding. (2) In the GPR/GoLoco-binding model, the GoLoco peptide interacts with both GTPase and helical domains of G α , docking its N-terminus within the SII/ α 3 site.³⁴ The C-terminus of GPR/GoLoco makes discriminate contacts with the helical domain of G α in the crystal structure, and functional studies using a series of

domain chimeras have demonstrated that these contacts are isoform-specific among G α i subunits.⁴⁰ However, the G α i1/G α s chimera C3, containing a G α s(s) helical domain and a G α i1 GTPase domain, shows no pull down on GSP or mGSP-1, indicating that our peptides do not recognize the G α s(s) helical domain. (3) In the effector-binding model, nonpolar effector residues dock within the hydrophobic pocket formed between the N-termini of SII(α 2) and α 3 helices (see asterisk in Fig. 1b). Specificity-determining contacts are made with the C-termini of these helices and the α 2- β 4 and α 3- β 5 effector loops of G α .^{11,12} The G α i1/G α s(s) chimera C4, containing the α 3 and α 3- β 5 and α 4- β 6 effector-binding loops of G α s(s), fully recapitulates G α s(s) pull down on GSP and recovers mGSP-1 binding. This result suggests that the GSP and mGSP-1 peptides discriminate G α targets in an effector-like binding mode via contacts with α 3 and/or the α 3- β 5 effector loop.

GSP and mGSP variants inhibit nucleotide exchange in G α s(s); GSP accelerates nucleotide exchange in G α i1

Finally, we wished to examine the effect of our selected peptides on nucleotide exchange. To do this, we have measured the GDP exchange rate in the presence and in the absence of GSP, mGSP-1, and mGSP-2 for both G α i1 and G α s(s) using two different assays (Fig. 6). The first assay measured GDP dissociation by monitoring [³⁵S]guanosine 5'-O-(3-thiotriphosphate) (GTP γ S) binding to G α under conditions where label binding is limited by GDP release. The second assay, employing [³²P]GTP, measured the steady-state GTP hydrolysis rate of G α under multiple turnover conditions where the rate of GTP hydrolysis is also limited by GDP release.

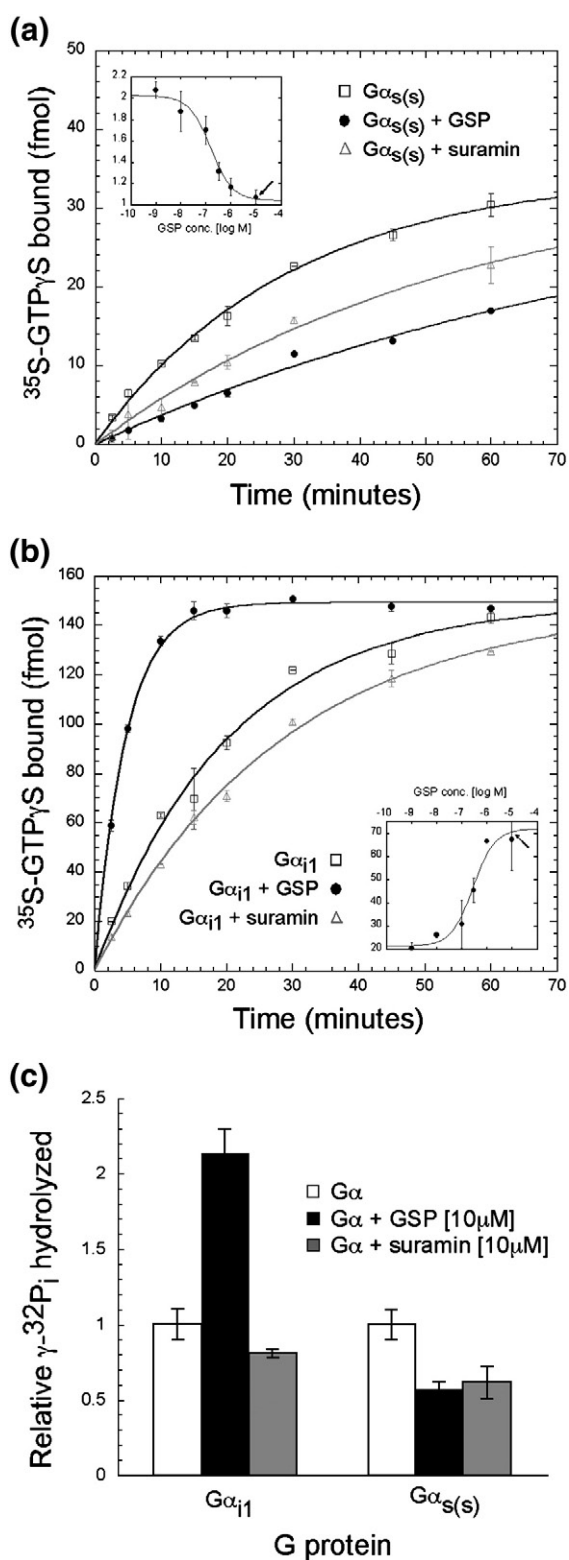


Fig. 6. GSP nucleotide exchange assays. (a) Time course of [³⁵S]GTP γ S binding to 50 nM G α s(s) at 20 °C in the presence of 10 μ M GSP or 10 μ M suramin. Data are fitted to a single exponential association curve to give apparent rates of GTP γ S association: G α s(s), 0.034 \pm 0.003 min⁻¹; +GSP, 0.011 \pm 0.004 min⁻¹; +suramin, 0.018 \pm 0.003 min⁻¹. Plots are normalized for maximum binding values, with error bars representing the SD of two measurements acquired during the same experiment. A dose-response curve is shown in the inset for 50 nM G α s(s) incubated with the indicated concentration of GSP for 2.5 min. Logistic fitting of the data gives an IC₅₀ value of 157 \pm 4 nM. Arrows indicate the concentration of peptide used in the time-course measurements. (b) Time course of [³⁵S]GTP γ S binding to 50 nM G α i1 at 30 °C in the presence of 10 μ M GSP or 10 μ M suramin. GTP γ S association rates: G α i1, 0.050 \pm 0.005 min⁻¹; +GSP, 0.214 \pm 0.007 min⁻¹; +suramin, 0.034 \pm 0.002 min⁻¹. The inset GSP-G α i1 dose-response curve gives an IC₅₀ value of 290 \pm 8 nM. (c) Steady-state hydrolysis is measured by inorganic phosphate [³²P_i] released from the reaction of 100 nM G α with [³²P]GTP in the presence of 10 μ M GSP or 10 μ M suramin. Error bars indicate the SD of multiple measurements.

Both assays demonstrate that GSP, mGSP-1, and mGSP-2 inhibit GDP exchange on G α s(s) (Fig. 6a and c). Incubating increasing amounts of GSP with G α s(s) inhibits [³⁵S]GTP γ S binding with an IC₅₀ of 157 nM, consistent with the 100-nM GSP-G α s(s) binding constant determined by SPR under similar, but not identical, conditions (Table 1). Under saturating GSP concentrations (10 μ M), the peptide slows GDP exchange by threefold, while similar kinetics are observed for mGSP-1 and mGSP-2 (Supplementary Fig. B). Thus, GSP, mGSP-1, and mGSP-2 have guanine nucleotide dissociation inhibitor activity against G α s(s).

To our surprise, the peptide GSP accelerates the rate of nucleotide exchange in G α i1. Under saturating GSP concentrations (10 μ M), the association rate of [³⁵S]GTP γ S on G α i1 is markedly increased compared to the protein alone (Fig. 6b). [³⁵S]GTP γ S binding measurements show that GSP acts as a guanine nucleotide exchange factor (GEF) for G α i1, accelerating the release of GDP by fourfold. The effective GSP concentration required for 50% maximal GEF activity is 290 nM, consistent with the dissociation constant of GSP-G α i1 (K_d =280 nM). Similar exchange measurements could not be made for mGSP-1 or mGSP-2, possibly due to the weak affinity of the peptides towards G α i1. The results demonstrate that GSP is bifunctional (has two activities)—with guanine-nucleotide-dissociation-inhibitor-like activity for G α s(s) and GEF activity for G α i1.

Interestingly, GSP is not alone in its bifunctional activity. The bee venom peptide melittin,⁴¹ as well as the nonspecific peptide KB-752 previously isolated by phage display,⁴² has been shown to have similar activity towards G α i1 and G α s(s). While melittin likely has a distinct functional mechanism, sequence conservation between GSP and KB-752 suggests that the two peptides bind G α i1/G α s(s) in a similar fashion. KB-752 shares a consensus EFL motif ('DFL') with selected peptides (Fig. 7a) and, like GSP, accelerates nucleotide exchange in G α i1 while inhibiting exchange in G α s(s), albeit at higher effective concentrations of 4–5 μ M.⁴²

Johnston *et al.* have solved a crystal structure of the KB-752-G α i1 complex, revealing peptide binding within the SII/ α 3 site of G α i1 (Fig. 7b).¹⁹ The F8 and L9 residues of KB-752 bury themselves within an invariant hydrophobic binding pocket composed of conserved residues R208, W211, I212, F215, L249, and I253 in G α i1. The EFL motifs of GSP and the mGSP variants presumably dock in a similar manner within the SII/ α 3 site. In the case of mGSP-1, the peptide C-terminus (residues 10–15), which is conserved among mGSP variants (Fig. 2c), is positioned to make discriminate contacts near the α 3- β 5 loop of G α s(s) in a cooperative fashion with α 3-binding mGSP-1 core residues.

Interestingly, the effector-binding model of peptide recognition presents a mechanistic rationale for the bifunctional activity of the GSP. Johnston *et al.* have proposed a mechanism for the G α i1 GEF activity of KB-752 wherein peptide-binding contacts peel back the switch-II lip of G α i1, facilitating nuc-

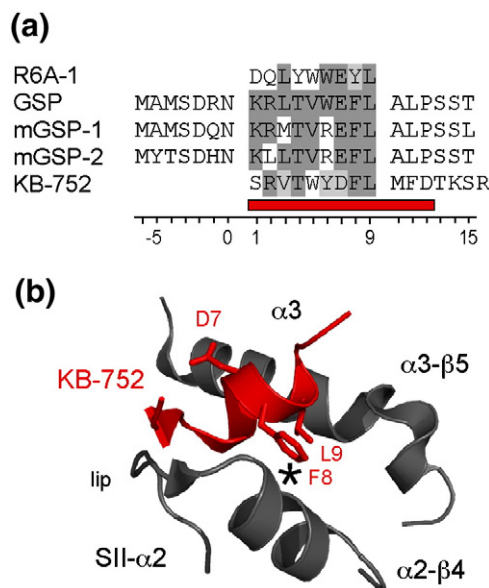


Fig. 7. α -binding 'EFL' peptides. (a) Sequence alignment of R6A-1, GSP, mGSP-1, mGSP-2, and KB-752: identical GSP core residues are highlighted in gray boxes, and conserved residues are highlighted in light gray; residues in the KB-752-G α i1 crystal structure are underlined in red. (b) Ribbon diagram of KB-752 (red) binding within the SII/ α 3 site of G α i1 (slate). The asterisk denotes an invariant hydrophobic binding pocket composed of G α i1 residues R208, W211, I212, F215, L49, and I253.¹¹ The structural image was made from PDB file 1Y3A.¹⁹ KB-752 consensus motif residues DFL are labeled (red) along with structural elements of G α i1 (slate).

leotide escape (Fig. 7b). This proposal is consistent with the G $\beta\gamma$ lever model of GPCR GEF activity⁴³ and, provided that GSP and KB-752 bind the SII lip in a similar manner, accounts for the G α i1 GEF activity of GSP. However, chimera discrimination experiments suggest that GSP binds the G α s(s) target at a shifted orientation within the SII/ α 3 site, accommodating specific contacts along the α 3 helix and the α 3- β 5 loop. Such a shift would disrupt contacts between GSP and the SII lip, blocking nucleotide release, which is consistent with the observed inhibition of GDP exchange in the GSP-G α s(s) complex.

Conclusions

We have reported the directed evolution of subclass-specific peptides targeting the highly conserved SII/ α 3 convergent binding surface of G α . A remarkable aspect of this work is our finding that the SII/ α 3 site, which is composed of nearly identical amino acids in the G α i1 and G α s(s) subunits, elicits an 8000-fold range of discrimination by related peptide ligands. This significant range of specificity argues that the surface conformation of the SII/ α 3 site, rather than its amino-acid identity, mediates ligand recognition. Such conformation-

specific class discrimination at the SII/ α 3 site has been noted in the effector binding specificity of G α s(s)^{11,12} and may also contribute to the specific binding of AC isoforms I-C₁, V-C₁, and VI-C₁ within the SII/ α 3 site of G α i1.⁴⁴ The work with G α suggests that it may be possible to discriminate binding hot spots on other highly conserved proteins in a similar conformation-specific manner, even in the case where crystallographic data indicate structural homology.

It was unclear, prior to selection, whether specific high-affinity targeting of G α subunit classes could be achieved using short peptide ligands. Our results demonstrate that linear peptides are well suited to the discrimination of G α , exhibiting 10- to 100-fold selectivities with affinity levels of between 60 nM and 300 nM. This finding should open doors to a number of applications. Fluorescent and luminescent biosensors have proven to be valuable molecules for the real-time tracking and visualization of G-protein signal transduction,⁴⁵⁻⁴⁷ and selected natural peptides could be employed in the development of these tools. Additionally, peptides with 10- to 100-fold binding specificities are viable capture reagents for chip-based proteomic analyses.⁴⁸

Our selected peptides are also capable of modulating G α protein function. The mGSPs, for instance, specifically target and inhibit G α s(s) at the convergent SII/ α 3-binding site of the subunit. It may, therefore, be possible to generate therapeutics targeted to the SII/ α 3 site for the treatment of various diseases caused by G α s activation.^{49,50} Constitutive activation of G α s by cholera toxin causes the pathophysiological symptoms of the disease. Separately, hyperactivating mutations of G α s can result in McCune-Albright syndrome and are oncogenic in various endocrine cancers.^{3,50} G α s oncogenes have been shown to increase tumorigenicity and metastasis,^{51,52} and recent identification of G α s-hyperactivating mutations in kidney cancer indicates that the subunit could be a therapeutic target in developed tumors.⁵³

Materials and Methods

Materials

The *Escherichia coli* strains BL21, BL21(DE3), and BL21-gold were obtained from Novagen (Madison, WI). The G-protein expression vector, NpT7-5-H6-TEV-G α i1, was generously provided by Prof. Roger K. Sunahara (University of Michigan). The *in vivo* biotinylation vector, pDW363, was kindly supplied by Dr. David S. Waugh (National Cancer Institute, Frederick, MD). Human cDNA clones encoding G proteins with the pcDNA3.1⁺ vector (Invitrogen) were obtained from the UMR cDNA Resource Center†. G α i1-rat and G α s(s)-bovine short form chimera constructs were generously provided by Prof. N. Artemyev (University of Iowa). The G α subunits used for the specificity profiles were i1, i2, i3, oA, q, 11, 15, s(s; short

isoform), s(l; long isoform), Olf, and 12. G α s(s) residues are referred to in the text with the G α s(l) numbering convention. DNA oligonucleotides were synthesized by Integrated DNA Technologies, Inc. (Coralville, IA). Modified and doped oligonucleotides, including pF30P, were synthesized at Keck Oligonucleotide Synthesis (New Haven, CT). DNA sequencing was performed by Laragen (Los Angeles, CA). L-[³⁵S]methionine (1175 Ci/mmol), [³⁵S]GTP γ S (1050 Ci/mmol), and [γ -³²P]GTP (6000 Ci/mmol) were purchased from MP Biomedicals (Irvine, CA). Restriction enzymes and T4 DNA ligase were obtained from New England Biolabs, Inc. (Beverly, MA). GSP, mGSP-1, mGSP-2, and R6A-1 peptides were purchased from BioSynthesis, Inc. (Lewisville, TX).

G α subunit cloning and expression

Cloning pDW363-H6-Gas(s)

pDW363-G α s(s) was modified with an amino-terminal hexahistidine tag by QuikChange (Stratagene) PCR using primers pDW363-H6-top (5' CTT TAA GAA GGA GAT ATA CAT ATG CAC CAC CAT CAC CAT CAC GCT GGA GGC CTG AAC GAT ATT TTC 3') and pDW363-H6-bottom (5' GAA AAT ATC GTT CAG GCC TCC AGC GTG ATG GTG ATG GTG CAT ATG TAT ATC TCC TTC TTA AAG 3'). A two-stage PCR protocol was adopted to mitigate the effects of primer-dimer formation (150 ng of template; 50 °C annealing temperature with a 12-min extension time at 68 °C; 3 rounds of amplification with primers separated; and 19 rounds with pooled reaction).⁵⁴ The pDW363-H6-G α s(s) sequence encodes H6-Nb-G α s(s), the G α s(s) protein with an N-terminal H6 hexahistidine tag followed by a peptide tag that is biotinylated *in vivo*.

Cloning reciprocal mutants

pcDNA3.1⁺ G α i1 was mutated at residue 206 (Ser206-Asp) by QuikChange (Stratagene) PCR using primers S206D-top (5' AAT GTT TGA TGT GGG AGG TCA GAG AGA TGA GCG GAA GAA G 3') and S206D-bottom (5' CTT CTT CCG CTC ATC TCT CTG ACC TCC CAC ATC AAA CAT T 3'). pcDNA3.1⁺ G α s(s) was mutated at residue 229 (Asp229Ser) by QuikChange (Stratagene) PCR using primers D229S-top (5' GGG TGG CCA GCG CTC TGA ACG CCG CAA G 3') and D229S-bottom (5' CTT GCG GCG TTC AGA GCG CTG GCC ACC C 3').

Expression of Gas(s)

G α s(s) was recombinantly expressed using previously published protocols, with some modifications.⁵⁵ A 100-ml enriched media culture [2% (wt/vol) tryptone, 1% (wt/vol) yeast extract, 0.5% (wt/vol) NaCl, 0.2% (vol/vol) glycerol, and 50 mM H₂PO₄ (pH 7.2), supplemented with 50 μ g/ml ampicillin and 50 μ M D-biotin] of *E. coli* BL21 (DE3) cells harboring pDW363-H6-G α s(s) was induced with 0.3 mM IPTG at OD₆₀₀=0.4, grown at 30 °C for 9 h, and pelleted by centrifugation. Pellets were rinsed with ddH₂O, snap-frozen in dry ice/ethanol, and stored at -80 °C overnight. Cell pellets were resuspended in 15 ml of T₅₀ β ₂₀P_{0.1} buffer [50 mM Tris-Cl (pH 8.0), 20 mM β -mercaptoethanol, and 0.1 mM phenylmethylsulfonyl fluoride], lysed by Emulsiflex at 5000 psi for 10 min, and centrifuged. Cleared lysate supernatant was applied to a 0.3-ml bed volume of Ni-NTA column (Qiagen) and preequilibrated with T₅₀ β ₂₀P_{0.1} (100 mM NaCl). The column was washed with 3 \times 2 ml of T₅₀ β ₂₀P_{0.1} (500 mM NaCl and 10 mM imidazole). Fractions were eluted into

† www.cdna.org

T₅₀P₂₀P_{0.1} [50 mM imidazole and 10% glycerol (vol/vol)], concentrated, exchanged with HGD buffer [50 mM Hepes (pH 7.5), 10% glycerol (vol/vol), and 1 mM DTT] using a Centriprep YM-10 concentrator, and stored at -80 °C. A 100-ml culture yielded 0.1 mg of N-terminally biotinylated G α s(s) (Nb-G α s(s)).

Expression of G α i1

Recombinant rat H6-TEV-G α i1 (N-terminal hexahistidine tag followed by a TEV protease cut site) was expressed as previously described.¹⁸ G α i1 was also expressed with an N-terminal peptide tag that is biotinylated *in vivo* (Nb-G α i1). A 120-ml LB culture (50 μ g/ml ampicillin and 50 μ M D-biotin) of *E. coli* BL21 cells harboring pDW363-G α i1 was induced with 1 mM IPTG at OD₆₀₀=0.6, grown at 30 °C for 6 h, and pelleted by centrifugation. Cell pellets were rinsed with ddH₂O, snap-frozen in dry ice/ethanol, and stored at -80 °C overnight. A 30-ml cell pellet was resuspended in 3 ml of BPER cell lysis reagent (Pierce) at room temperature. The lysate was cleared by centrifugation and incubated with 0.4 ml of neutravidin agarose at 4 °C for 1 h. The beads were washed five times with wash buffer [1 \times phosphate-buffered saline (PBS), 3 μ M GDP, 2 mM DTT, and 0.5% Tween-20 (vol/vol)] to generate G α i1 beads.

mRNA display: Template construction and selection

Construction of the core motif R6A-1 library has been described previously.²⁰ The GSP library was designed in a similar fashion to incorporate roughly 50% degeneracy per amino-acid residue.⁵⁶ The antisense DNA oligo 115.2 [5' AGC AGA CAG ACT AGT GTA ACC GCC 624 621 621 622 612 623 612 211 543 531 613 624 612 632 544 244 632 243 621 514 623 CAT TGT AAT TGT AAA TAG TAA TTG TCC C 3'; numbers denote deoxynucleoside 5'-triphosphate mixtures: (1) 70% A, 10% G, 10% C, 10% T; (2) 70% G, 10% A, 10% C, 10% T; (3) 70% C, 10% A, 10% G, 10% T; (4) 70% T, 10% A, 10% G, 10% C; (5) 90% C, 10% G; (6) 50% G, 50% C] was synthesized by Keck Oligonucleotide Synthesis. This oligo was PCR-amplified with the forward primer 47T7FP (5' GGA TTC TAA TAC GAC TCA CTA TAG GGA CAA TTA CTA TTT ACA ATT AC 3') and the reverse primer 22.9 (5' AGC AGA CAG ACT AGT GTA ACC G 3') to generate the doped GSP library. The purified double-stranded DNA (dsDNA) construct contained a T7 promoter, an untranslated region, and an open reading frame containing a 3' constant sequence encoding the peptide QLRNSCA. Sequencing of pool 0 demonstrated ~50% degeneracy of the library per doped amino-acid position. The expected amino acid distribution of the GSP library is included in Supplemental Material.

All steps in the mRNA display selection cycle, with the exception of the G α binding step, were performed as previously described.¹⁸ The G α s(s) beads were prepared immediately prior to use in selections. Nb-G α s(s) (15–30 μ g) was rotated with a 30- μ l bed volume of neutravidin agarose (Pierce) in 0.5 ml of wash buffer [1 \times PBS, 3 μ M GDP, 2 mM DTT, and 0.5% Tween-20 (vol/vol)] at 4 °C for 1 h. Beads were washed with wash buffer and resuspended in binding buffer [25 mM Hepes-KOH (pH 7.5), 150 mM NaCl, 1 mM β -mercaptoethanol, 10 μ M GDP, 1 mM ethylenediaminetetraacetic acid (EDTA), 5 mM MgCl₂, and 0.05% (vol/vol) Tween-20] supplemented with 1 mM D-biotin (0.1 mM) and rotated for an additional 10 min to block biotin-binding sites. Beads were then

washed thoroughly with selection buffer [25 mM Hepes-KOH (pH 7.5), 150 mM NaCl, 1 mM β -mercaptoethanol, 10 μ M GDP, 1 mM EDTA, 5 mM MgCl₂, 0.05% (vol/vol) Tween-20, 0.05% (wt/vol) bovine serum albumin (BSA) (electrophoresis-grade; Sigma), and 1 μ g/ml yeast tRNA (Roche Diagnostics Corp., Indianapolis, IN)] and rotated with reverse transcription (RT) fusions in 1 ml of selection buffer at 4 °C for 1 h. The matrix was then washed with 4 \times 0.5 ml of selection buffer followed by 2 \times 0.5 ml of binding buffer. Bound fusions were eluted with 2 \times 0.1 ml of 0.15% (wt/vol) SDS using a 0.45- μ m centrifuge tube filter. SDS was removed using SDS-OUT (Pierce) following the manufacturer's specifications, and cDNA was ethanol-precipitated with linear acrylamide (Ambion). PCR amplification of the cDNA with primers 47T7FP and 22.9 generated the dsDNA template for the next round of selection. DNA templates could also be cloned into pDW363C for sequencing.

Additional negative G α i1 selective pressures were applied during the maturation selection. RT fusions were sieved through a column of G α i1 beads (0.3-ml bed volume equilibrated in selection buffer) prior to incubation with G α s(s) beads. Incubation of the presieved RT fusion and G α s(s) beads was performed in selection buffer supplemented with soluble G α i1 competitor at a concentration ranging from 10 μ g/ml in round 1 (R1) of selection to 20 μ g/ml (R2), to 40 μ g/ml (R3–R6). Washes of the G α s(s) beads after incubation with presieved RT fusions were conducted in selection buffer supplemented with 20 μ g/ml soluble G α i1 competitor (R3–R6). Binding assays between [³⁵S]Met-peptide fusions and G α i1 beads or G α s(s) beads were performed as previously described.¹⁸

Cloning and expression of selected peptides

Selected pools were cloned into the biotinylation vector pDW363C²⁹ for sequencing and expression. Pool dsDNA was PCR-amplified using universal primer 29.4 (5' TGA AGT CTG GAG TAT TTA CAA TTA CAA TG 3') and reverse primer 22.9 (5' AGC AGA CAG ACT AGT GTA ACC G 3'), digested with BpmI/SpeI, and ligated to pDW363C (digested with BseRI/SpeI). Ligations were digested with KpnI to reduce vector-only contaminant, transformed into the BL21-gold (Stratagene) *E. coli* cell line, and plated on LB-Amp. Individual colonies were picked for sequencing.

Selected peptides were expressed as MBP fusions using the *in vivo* biotinylation system pDW363C [Nb-(Factor Xa site)-peptide-MBP]. Expression and cell lysate preparation of pDW363C clones, as well as MBP and R6A-MBP controls, were performed as described above. Nb-peptide-MBP was purified directly onto neutravidin agarose to generate peptide beads for the G α binding screen and G α specificity profiles. For applications requiring removal of the biotin tag (Nb) from the peptide, Factor Xa was used following previously published protocols.¹⁸ Briefly, cleared lysate was purified on streptavidin Sepharose (high-performance; Amersham) and washed five times with pDW buffer [50 mM Hepes-KOH (pH 7.5), 200 mM NaCl, 1 mM EDTA, and 0.1% Triton X-100] followed by washes (two times) with Xa buffer [50 mM Hepes-KOH (pH 7.5), 150 mM NaCl, and 1 mM CaCl₂]. Protein was incubated overnight with Factor Xa (20 U; Amersham) in Xa buffer at room temperature and eluted with pDW buffer. Factor Xa was removed with *p*-aminobenzamidine agarose (Sigma). Purified proteins were desalted and concentrated in a Centriprep YM-30 into 1 \times PBS.

Library complexity and selected peptide sequence probabilities

The complexity of R6A-1 and GSP libraries was determined to be 1.6×10^{13} and 2.5×10^{12} peptide sequences in their respective pool 0. This value was calculated by dividing the radioactive counts [counts per minute (cpm)] of dT-purified mRNA-peptide fusions by cpm per molecule of the incorporated [^{35}S]methionine and corrected for the incidence of methionine in each peptide (R6A-1 library: 1.48 Met/peptide; GSP library: 1.66 Met/peptide).⁵⁶ Sixty discrete peptide-MBP clones were screened from both round 8 of the positive selection and round 6 of the maturation selection.

Analysis of the GSP sequence

The likelihood of finding the GSP core sequence in our R6A-1 library was calculated from the amino-acid doping probability at each residue in the peptide. The GSP core sequence [K1 (0.7%), R2 (7.9%), L3 (52.5%), T4 (1.0%), V5 (1.0%), W6 (44.1%), E7 (44.1%), F8 (6.3%), L9 (52.5%)] has an incidence of 1.9×10^{-10} . Correcting for the occurrence of stop codons, there should be 773 full-length copies of the GSP core sequence in the R6A-1 library pool 0.

Analysis of mGSP sequences

Sequence analysis was performed on a sample of 11 mGSP sequences shown to have the greatest $\text{G}\alpha\text{s}(\text{s})$ binding specificity in the $\text{G}\alpha$ binding screen. These mGSP sequences have an average mutational distance of 5.7 ± 1.3 mutated residues from GSP. Using equations developed by Knight and Yarus to evaluate doped library sampling probabilities, we calculate that, in the GSP library pool 0, which has a complexity of 2.5 trillion peptides, a mutational distance of 5.7 residues is covered at a copy number of 1.0.⁵⁷ This value is, however, based on the inaccurate assumption that each conserved amino-acid residue is capable of being mutated to each of the 19 other amino acids at the same frequency. Based on the doping scheme of the GSP-1 library, the probability of generating a discrete mutation at a doped residue ranges from 0.5% to 7%.⁵⁶ If we subtract the 10 most unlikely mutations, comprising a 5% probability, the copy number increases to 4.4 copies.

$\text{G}\alpha$ binding screen and specificity profile assay

[^{35}S]Met-labeled G-protein subunits were translated discretely in coupled transcription/translation reactions using the TNT reticulocyte lysate system (T7 promoter; Promega, Madison, WI). Typically 0.3–1.0 μg of plasmid DNA and 25 μCi of L-[^{35}S]methionine were used per 25- μl reaction. Reactions were desalted and exchanged using MicroSpin G-25 columns (GE Healthcare) into buffer [50 mM Hepes-KOH (pH 7.5), 6 mM MgCl_2 , 75 mM sucrose, 1 mM EDTA, 1 μM GDP, and 0.5% (vol/vol) Tween-20], and reaction yields were quantitated by trichloroacetic acid precipitation of a 2- μl aliquot of each reaction.

The $\text{G}\alpha$ interaction assay was performed as described previously.²⁹ Individual binding reactions were assembled with equivalent aliquots of desalted $\text{G}\alpha$ subunits in 0.5 ml of binding buffer [0.5% (wt/vol) BSA] containing 10 μl of peptide beads. After rotation of the beads at 4 °C for 1 h, they were washed three times with 0.5 ml of binding

buffer using a 0.45- μm spin filter tube and transferred to a vial for scintillation counting. Assays with AlF_4 were performed similarly, except that binding buffer was supplemented with 10 mM NaF and 25 μM AlCl_3 .

Binding analysis by SPR

Kinetic measurements were conducted at 25 °C on a Biacore 2000 instrument (Biacore, Inc., Piscataway, NJ), as described previously.¹⁸ Briefly, Nb-G $\alpha\text{s}(\text{s})$ and Nb-G $\alpha\text{i}1$ were immobilized on research-grade streptavidin sensor chips at a surface density of ~ 1000 response units. A concentration series (0 nM, 10 nM, 30 nM, 90 nM, 270 nM, 810 nM, and 2430 nM) of each peptide analyte in modified HBS-EP running buffer [10 mM Hepes (pH 7.4), 150 mM NaCl, 3 mM EDTA, 0.005% (vol/vol) Tween-20, 2 mM MgCl_2 , 30 μM GDP, 0.05% (wt/vol) BSA, and 0–0.5% dimethyl sulfoxide] was injected across the chip for 2 min at 100 $\mu\text{l}/\text{min}$, followed by a 6-min dissociation period. A negative control surface without immobilized $\text{G}\alpha$ was used to monitor background binding of the analyte. K_d values for peptides were calculated from rates determined by CLAMP. Additionally, K_d values were determined from equilibrium binding responses using Scrubber. These equilibrium fits produced similar results, with K_d values within 50% of those shown.

$\text{G}\alpha$ nucleotide cycle assays

GTP γS exchange assays were performed using a nitrocellulose filter binding method⁵⁸ at either 20 °C (G $\alpha\text{s}(\text{s})$) or 30 °C (G $\alpha\text{i}1$). Briefly, $\text{G}\alpha$ was diluted into HEDT buffer [50 mM Hepes-NaOH (pH 7.6), 1 mM EDTA, 1 mM DTT, and 0.01% Tween-20] to a final concentration of 250 nM (1 pmol/10 μl assay) on ice. The reaction was started by adding 4 vol (40 $\mu\text{l}/\text{assay}$) of reaction buffer [50 mM Hepes-NaOH (pH 7.6), 1 mM EDTA, 1 mM DTT, 12.5 mM MgSO_4 , 0.2–1.2 μM [^{35}S]GTP γS (50–200 cpm/fmol), and 0.01% Tween-20] with or without test peptide. The reactions were stopped by withdrawing duplicate aliquots (50 $\mu\text{l}/\text{assay}$), diluting these into 10 ml of ice-cold stop buffer [Tris-HCl (pH 8.0), 100 mM NaCl, 25 mM MgCl_2 , and 100 μM GTP], and immediately filtering over HA-85 nitrocellulose membranes (Whatman). Equilibrium experiments were conducted similarly, with the exception that $\text{G}\alpha$ subunits were preincubated for 10 min with or without peptide on ice prior to initiating reactions. Data from kinetic experiments were processed by nonlinear least squares curve fitting to a pseudo-first-order association rate. Concentration response curves were fitted to a three-parameter logistic equation. All measurements were performed multiple times.

Steady-state [γ - ^{32}P]GTP assays were undertaken using a charcoal-precipitation-based method⁵⁹ at either 20 °C (G $\alpha\text{s}(\text{s})$) or 30 °C (G $\alpha\text{i}1$). $\text{G}\alpha$ proteins were diluted on ice to 200 nM (2 \times desired concentration) in assay buffer [20 mM NaHepes (pH 8.0), 100 mM NaCl, 1 mM EDTA, 2 mM MgCl_2 , 1 mM DTT, and 0.05% Tween-20]. GTPase reactions were initiated by the addition of an equal volume of assay buffer containing a 2 \times concentration of 0.3–1 μM [γ - ^{32}P]GTP (1000–3000 cpm/fmol) \pm peptide. Duplicate aliquots (50 μl) were removed at timed intervals and quenched with 900 μl of ice-cold 5% (wt/vol) activated charcoal in 50 mM NaH_2PO_4 . Quenched reactions were centrifuged for 10 min at 8000g, and duplicate 100- μl aliquots of the resultant supernatant were subjected to scintillation counting to quantify released [^{32}P].

Acknowledgements

We would like to thank N.O. Artemyev for providing the $G\alpha 11/G\alpha s(s)$ chimeras; R.T. Sunahara for the TEV protein expression vector; D.S. Waugh for the original pDW363 vector; and P.J. Bjorkman for the use of the Biacore 2000 instrument. Thanks to T.T. Takahashi for helpful discussions and to anonymous reviewers for their criticisms. This work was supported by grants to R.W.R. from the National Institutes of Health (R01 GM 60416) and the Charles Lee Powell Foundation.

Supplementary Data

Supplementary data associated with this article can be found, in the online version, at [doi:10.1016/j.jmb.2008.01.032](https://doi.org/10.1016/j.jmb.2008.01.032)

References

- Hopkins, A. L. & Groom, C. R. (2002). The druggable genome. *Nat. Rev. Drug Discov.* **1**, 727–730.
- Neves, S. R., Ram, P. T. & Iyengar, R. (2002). G protein pathways. *Science*, **296**, 1636–1639.
- Wetschurck, N. & Offermanns, S. (2005). Mammalian G proteins and their cell type specific functions. *Physiol. Rev.* **85**, 1159–1204.
- Freissmuth, M., Waldhoer, M., Bofill-Cardona, E. & Nanoff, C. (1999). G protein antagonists. *Trends Pharmacol. Sci.* **20**, 237–245.
- Holler, C., Freissmuth, M. & Nanoff, C. (1999). G proteins as drug targets. *Cell. Mol. Life Sci.* **55**, 257–270.
- Arkin, M. R. & Wells, J. A. (2004). Small-molecule inhibitors of protein–protein interactions: progressing towards the dream. *Nat. Rev. Drug Discov.* **3**, 301–317.
- Chenna, R., Sugawara, H., Koike, T., Lopez, R., Gibson, T. J., Higgins, D. G. & Thompson, J. D. (2003). Multiple sequence alignment with the Clustal series of programs. *Nucleic Acids Res.* **31**, 3497–3500.
- Sunahara, R. K., Tesmer, J. J., Gilman, A. G. & Sprang, S. R. (1997). Crystal structure of the adenylyl cyclase activator $G_{\alpha s}$. *Science*, **278**, 1943–1947.
- Birnbaumer, L. (2004). Signal transduction by G proteins: basic principles, molecular diversity, and structural basis of their actions. In *Handbook of Cell Signaling* (Bradshaw, R. A. & Dennis, E. A., eds), Academic, Boston, MA.
- Blumer, J. B., Smrcka, A. V. & Lanier, S. M. (2007). Mechanistic pathways and biological roles for receptor-independent activators of G-protein signaling. *Pharmacol. Ther.* **113**, 488–506.
- Tesmer, V. M., Kawano, T., Shankaranarayanan, A., Kozasa, T. & Tesmer, J. J. (2005). Snapshot of activated G proteins at the membrane: the $G\alpha_q$ -GRK2- $G\beta\gamma$ complex. *Science*, **310**, 1686–1690.
- Chen, Z., Singer, W. D., Sternweis, P. C. & Sprang, S. R. (2005). Structure of the p115RhoGEF rgRGS domain- $G\alpha 13/i1$ chimera complex suggests convergent evolution of a GTPase activator. *Nat. Struct. Mol. Biol.* **12**, 191–197.
- Johnston, C. A., Lobanova, E. S., Shavkunov, A. S., Low, J., Ramer, J. K., Blaesusius, R. et al. (2006). Minimal determinants for binding activated $G\alpha$ from the structure of a $G\alpha(i1)$ -peptide dimer. *Biochemistry*, **45**, 11390–11400.
- Clackson, T. & Wells, J. A. (1995). A hot spot of binding energy in a hormone–receptor interface. *Science*, **267**, 383–386.
- DeLano, W. L. (2002). Unraveling hot spots in binding interfaces: progress and challenges. *Curr. Opin. Struct. Biol.* **12**, 14–20.
- Kreutz, B., Yau, D. M., Nance, M. R., Tanabe, S., Tesmer, J. J. & Kozasa, T. (2006). A new approach to producing functional $G\alpha$ subunits yields the activated and deactivated structures of $G\alpha(12/13)$ proteins. *Biochemistry*, **45**, 167–174.
- Ma, B., Wolfson, H. J. & Nussinov, R. (2001). Protein functional epitopes: hot spots, dynamics and combinatorial libraries. *Curr. Opin. Struct. Biol.* **11**, 364–369.
- Ja, W. W. & Roberts, R. W. (2004). *In vitro* selection of state-specific peptide modulators of G protein signaling using mRNA display. *Biochemistry*, **43**, 9265–9275.
- Johnston, C. A., Willard, F. S., Jezyk, M. R., Fredericks, Z., Bodor, E. T., Jones, M. B. et al. (2005). Structure of $G\alpha(i1)$ bound to a GDP-selective peptide provides insight into guanine nucleotide exchange. *Structure*, **13**, 1069–1080.
- Ja, W. W., Wiser, O., Austin, R. J., Jan, L. Y. & Roberts, R. W. (2006). Turning G proteins on and off using peptide ligands. *ACS Chem. Biol.* **1**, 570–574.
- Roberts, R. W. & Szostak, J. W. (1997). RNA–peptide fusions for the *in vitro* selection of peptides and proteins. *Proc. Natl. Acad. Sci. USA*, **94**, 12297–12302.
- Takahashi, T. T., Austin, R. J. & Roberts, R. W. (2003). mRNA display: ligand discovery, interaction analysis and beyond. *Trends Biochem. Sci.* **28**, 159–165.
- Wilson, D. S., Keefe, A. D. & Szostak, J. W. (2001). The use of mRNA display to select high-affinity protein-binding peptides. *Proc. Natl. Acad. Sci. USA*, **98**, 3750–3755.
- Keefe, A. D. & Szostak, J. W. (2001). Functional proteins from a random-sequence library. *Nature*, **410**, 715–718.
- Austin, R. J., Xia, T., Ren, J., Takahashi, T. T. & Roberts, R. W. (2002). Designed arginine-rich RNA-binding peptides with picomolar affinity. *J. Am. Chem. Soc.* **124**, 10966–10967.
- Raffler, N. A., Schneider-Mergener, J. & Famulok, M. (2003). A novel class of small functional peptides that bind and inhibit human alpha-thrombin isolated by mRNA display. *Chem. Biol.* **10**, 69–79.
- Getmanova, E. V., Chen, Y., Bloom, L., Gokemeijer, J., Shamah, S., Warikoo, V. et al. (2006). Antagonists to human and mouse vascular endothelial growth factor receptor 2 generated by directed protein evolution *in vitro*. *Chem. Biol.* **13**, 549–556.
- Ja, W. W., West, A. P., Jr., Delker, S. L., Bjorkman, P. J., Benzer, S. & Roberts, R. W. (2007). Extension of *Drosophila melanogaster* life span with a GPCR peptide inhibitor. *Nat. Chem. Biol.* **3**, 415–419.
- Ja, W. W., Adhikari, A., Austin, R. J., Sprang, S. R. & Roberts, R. W. (2005). A peptide core motif for binding to heterotrimeric G protein alpha subunits. *J. Biol. Chem.* **280**, 32057–32060.
- Willard, F. S. & Siderovski, D. P. (2006). The R6A-1 peptide binds to switch II of $G\alpha 11$ but is not a GDP-dissociation inhibitor. *Biochem. Biophys. Res. Commun.* **339**, 1107–1112.
- Dalby, P. A. (2003). Optimising enzyme function by directed evolution. *Curr. Opin. Struct. Biol.* **13**, 500–505.
- Tesmer, J. J., Berman, D. M., Gilman, A. G. & Sprang, S. R. (1997). Structure of RGS4 bound to AIF₄-activated $G(i\alpha 1)$: stabilization of the transition state for GTP hydrolysis. *Cell*, **89**, 251–261.

33. Slep, K. C., Kercher, M. A., He, W., Cowan, C. W., Wensel, T. G. & Sigler, P. B. (2001). Structural determinants for regulation of phosphodiesterase by a G protein at 2.0 Å. *Nature*, **409**, 1071–1077.
34. Kimple, R. J., Kimple, M. E., Betts, L., Sondek, J. & Siderovski, D. P. (2002). Structural determinants for GoLoco-induced inhibition of nucleotide release by G α subunits. *Nature*, **416**, 878–881.
35. Wall, M. A., Posner, B. A. & Sprang, S. R. (1998). Structural basis of activity and subunit recognition in G protein heterotrimers. *Structure*, **6**, 1169–1183.
36. Natochin, M. & Artemyev, N. O. (1998). Substitution of transducin ser202 by asp abolishes G-protein/RGS interaction. *J. Biol. Chem.* **273**, 4300–4303.
37. Woulfe, D. S. & Stadel, J. M. (1999). Structural basis for the selectivity of the RGS protein, GAIP, for G α i family members. Identification of a single amino acid determinant for selective interaction of G α i subunits with GAIP. *J. Biol. Chem.* **274**, 17718–17724.
38. Natochin, M., Gasimov, K. G. & Artemyev, N. O. (2002). A GPR–protein interaction surface of G α i (alpha): implications for the mechanism of GDP-release inhibition. *Biochemistry*, **41**, 258–265.
39. Zheng, B., Ma, Y. C., Ostrom, R. S., Lavoie, C., Gill, G. N., Insel, P. A. *et al.* (2001). RGS-PX1, a GAP for G α S and sorting nexin in vesicular trafficking. *Science*, **294**, 1939–1942.
40. Mittal, V. & Linder, M. E. (2004). The RGS14 GoLoco domain discriminates among G α i isoforms. *J. Biol. Chem.* **279**, 46772–46778.
41. Fukushima, N., Kohno, M., Kato, T., Kawamoto, S., Okuda, K., Misu, Y. & Ueda, H. (1998). Melittin, a metabostatic peptide inhibiting Gs activity. *Peptides*, **19**, 811–819.
42. Johnston, C. A., Ramer, J. K., Blaesius, R., Fredericks, Z., Watts, V. J. & Siderovski, D. P. (2005). A bifunctional G α i/G α s modulatory peptide that attenuates adenylyl cyclase activity. *FEBS Lett.* **579**, 5746–5750.
43. Rondard, P., Iiri, T., Srinivasan, S., Meng, E., Fujita, T. & Bourne, H. R. (2001). Mutant G protein alpha subunit activated by G β γ : a model for receptor activation? *Proc. Natl Acad. Sci. USA*, **98**, 6150–6155.
44. Dessauer, C. W., Tesmer, J. J., Sprang, S. R. & Gilman, A. G. (1998). Identification of a G α i binding site on type V adenylyl cyclase. *J. Biol. Chem.* **273**, 25831–25839.
45. Janetopoulos, C., Jin, T. & Devreotes, P. (2001). Receptor-mediated activation of heterotrimeric G-proteins in living cells. *Science*, **291**, 2408–2411.
46. Hamdan, F. F., Audet, M., Garneau, P., Pelletier, J. & Bouvier, M. (2005). High-throughput screening of G protein-coupled receptor antagonists using a bioluminescence resonance energy transfer 1-based beta-arrestin2 recruitment assay. *J. Biomol. Screen*, **10**, 463–475.
47. Gibson, S. K. & Gilman, A. G. (2006). G α and G β subunits both define selectivity of G protein activation by alpha2-adrenergic receptors. *Proc. Natl Acad. Sci. USA*, **103**, 212–217.
48. Phelan, M. L. & Nock, S. (2003). Generation of bioreagents for protein chips. *Proteomics*, **3**, 2123–2134.
49. Weinstein, L. S., Liu, J., Sakamoto, A., Xie, T. & Chen, M. (2004). Minireview: GNAS: normal and abnormal functions. *Endocrinology*, **145**, 5459–5464.
50. Spiegel, A. M. & Weinstein, L. S. (2004). Inherited diseases involving G proteins and G protein-coupled receptors. *Annu. Rev. Med.* **55**, 27–39.
51. Chien, J., Wong, E., Nikes, E., Noble, M. J., Pantazis, C. G. & Shah, G. V. (1999). Constitutive activation of stimulatory guanine nucleotide binding protein (G(S) alphaQL)-mediated signaling increases invasiveness and tumorigenicity of PC-3M prostate cancer cells. *Oncogene*, **18**, 3376–3382.
52. Regnaud, K., Nguyen, Q. D., Vakaet, L., Bruyneel, E., Launay, J. M., Endo, T. *et al.* (2002). G-protein alpha(olf) subunit promotes cellular invasion, survival, and neuroendocrine differentiation in digestive and urogenital epithelial cells. *Oncogene*, **21**, 4020–4031.
53. Kalfa, N., Lumbroso, S., Boulle, N., Guiter, J., Soustelle, L., Costa, P. *et al.* (2006). Activating mutations of G α in kidney cancer. *J. Urol.* **176**, 891–895.
54. Wang, W. & Malcolm, B. A. (1999). Two-stage PCR protocol allowing introduction of multiple mutations, deletions and insertions using QuikChange site-directed mutagenesis. *Biotechniques*, **26**, 680–682.
55. Lee, E., Linder, M. E. & Gilman, A. G. (1994). Expression of G-protein alpha subunits in *Escherichia coli*. *Methods Enzymol.* **237**, 146–164.
56. LaBean, T. H. & Kauffman, S. A. (1993). Design of synthetic gene libraries encoding random sequence proteins with desired ensemble characteristics. *Protein Sci.* **2**, 1249–1254.
57. Knight, R. & Yarus, M. (2003). Analyzing partially randomized nucleic acid pools: straight dope on doping. *Nucleic Acids Res.* **31**, e30.
58. Nanoff, C., Kudlacek, O. & Freissmuth, M. (2002). Development of Gs-selective inhibitory compounds. *Methods Enzymol.* **344**, 469–480.
59. Ross, E. M. (2002). Quantitative assays for GTPase-activating proteins. *Methods Enzymol.* **344**, 601–617.